Chapter X[1]

Quality of raster data

1. Introduction

The quality of raster data measures the ability of each pixel to provide users with a reliable spectral and thematic information together with a known Earth location.

This quality is a necessary condition that will enable:

– processing large areas, seamlessly assembling data acquired at different period of time (mosaics, synthesis);

- monitoring geophysical measurements overtime (multi-temporal analysis);

- merging data acquired from different instruments to derive new thematic information with better accuracy.

Quality of raster data is processed in two distinct domains:

– geometric qualification, and

– radiometric qualification.

Activities performed in these two domains involve different methods and are generally operated by experts providing specific knowledge: - cartography and geodesy for the first ones, - radiative transfer physics and thematic skills for the second ones.

[1] Chapter edited by Serge RIAZANOFF for the « Geometry quality » section and Richard SANTER for the « Radiometry quality ».

To enable radiometric qualification, for example operating validation techniques from measurements of another instrument, it is required to first “geolocate” (we also say “collocate”) Earth observation data. This is the reason while the geometry qualification shall be performed *before* the radiometry qualification.

2. Geometry quality

Geometric processing performed on one image transforms it, and makes it conform withto a cartographic reference system. The product of such a transformation is called a *spacemap*.

Figure X.1. Orthorectified aerial photograph superposed on a map.
(Courtesy TTI Productions).

Many factors impact on the quality of the acquired image; these are presented in this section.

After having provided some definitions and setting a theoretical framework, various geometry defects will be presented, complemented by the presentation of the two most used methods to verify image geometry.

2.1. *Image reference system and modelling of the viewing geometry*

2.1.1. Image reference system in matrix representation

One image is made up of m lines, each one containing n points (or pixels), and is generally stored in one or more files which first point matches the upper-left corner of the image. In order to comply with this constraint and to handle a direct base (according to a mathematical point of view), it is recommended to use a Cartesian reference system giving first the coordinate l of the line (see figure X.2).

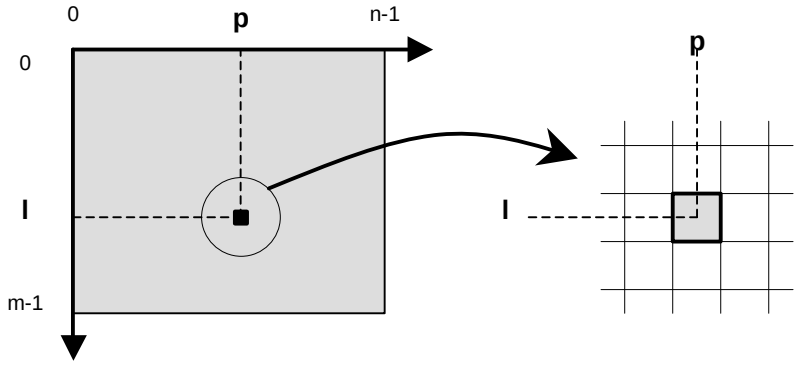

Figure X.2. *Image reference system and elementary grid-cell.*

Point (l,p) of an image has a footprint on the ground which is represented by a square. Such a footprint defines an elementary grid-cell (see its definition in the next section) that may be represented on the Earth surface, and for which may be provided its geodetic coordinates. Common usage is to consider these coordinates at the centre of the grid-cell. Nevertheless, some geocoded images consider that the geodetic coordinates refer to the upper-left corner of the grid-cell.

Any uncertainty regarding the location within the grid-cell (centre or corner) of the geodetic coordinates could lead to a systematic error of 0.5 pixels along the two directions (i.e. a total of $\sqrt{2}/2$ pixels).

Note also that a square footprint representation is intrinsically improper because the radiometry measured at one point in fact corresponds to the integration of backscattered energies across a surface (called “point spread distribution”) which almost never matches a square pattern (see figure X.3).

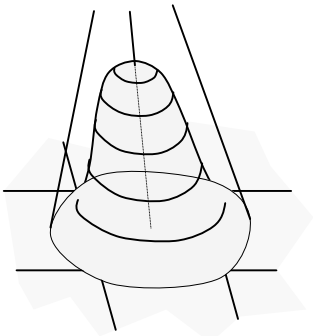

Figure X.3. *Point Spread Distribution (PSD) over an elementary grid-cell.*

2.1.2. *Direct and inverse localisation*

Modelling the geometry of a Earth observation image consists in defining a relation linking any point (l,p) of the image to geodetic coordinates (λ,φ) expressed in a reference system attached to the Earth[2].

To enable using a georeferenced image, it is necessary to know the *direct localisation function* f (more generally called *direct deformation* model) and/or the *inverse localisation function* f^{-1} (also called *inverse deformation model*) that are mathematical formulae given in the generic form:

direct localisation function $f(l, p, h, var) = (l, j)$ [X.1]

inverse localisation function $f^{-1}(l, j, h, var) = (l, p)$ [X.2]

Where

(l,p)	are the coordinates of the point in the image,
(l, j)	are the geodetic coordinates of this point on Earth surface,
h	matches the altitude of the point above the Earth surface,
var	are auxiliary variables, private resources required by the model (for example the coordinates of the viewing vector, the resolution…).

[2] In this chapter, (λ,φ) denotes the geodetic coordinates that usually match the (longitude, latitude) couple without considering the case of coordinates (X,Y) expressed in other geodetic reference systems like for example Lambert or UTM. Conversion between these coordinate systems is performed using standard formulae of projection change; the description of which is out the scope of this book.

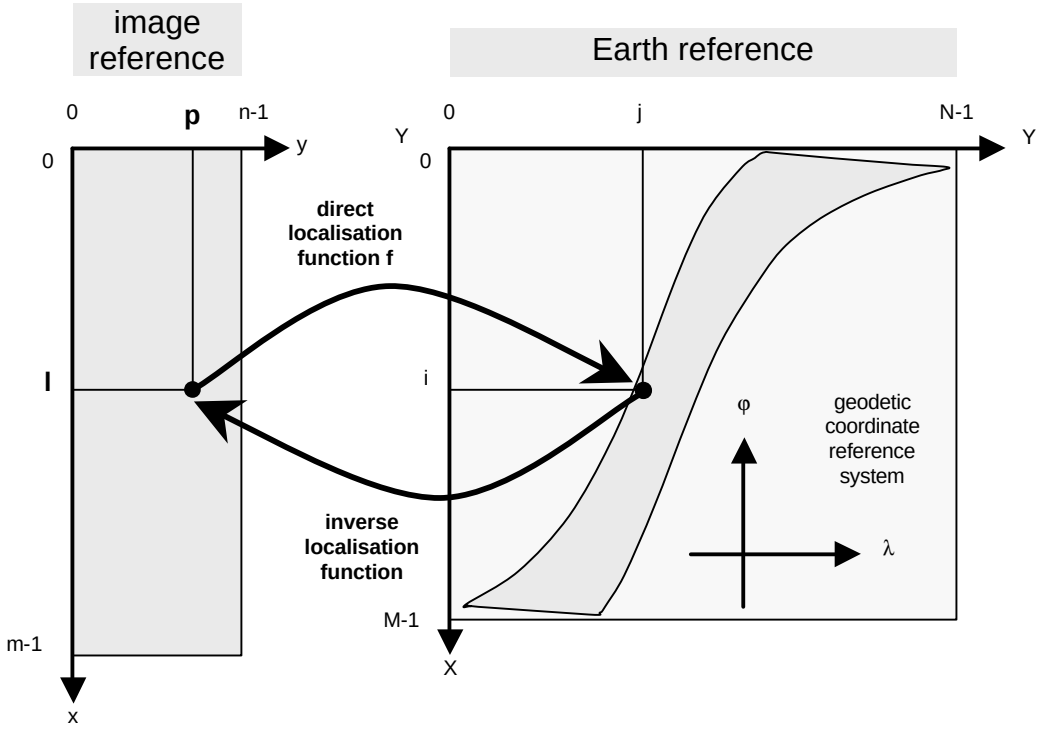

Figure X.4. *Image and terrestrial reference .frames.*

2.1.3. Geometric transforms of images

As seen previously, the *direct localisation function* may be used to determine the point location in a terrestrial reference frames but may also be used, combined with the *inverse localisation function*, to transform the image geometry (we sometimes say *to* (*re)project*) into a terrestrial frame, producing a spacemap in a classical projection (see figure X.4).

The *direct localisation function* enables projecting the four corners of the original image (or all the points of the image boundary when the transform is complex as shown in figure X.4) to determine the size and the terrestrial location (footprint) of the destination image.

The *inverse location function* plays an essential role while reprojecting the image because it enables constructing the destination image point by point, retrieving for each point (i,j) of this destination image the coordinates (x,y) of the parent point in the original image.

Coordinates (x,y) are rarely integers and it is therefore necessary to interpolate the value of the radiometry R(i,j) that will be set in the destination image. Choice of the *interpolation method* (nearest neighbour, bi-linear, bi-cubic, sinus cardinal…) is an important criteria that should be taken into account while evaluating the quality of raster data.

2.1.4. *Acquisition models*

2.1.4.1. Scanner documents

In the framework of projects dealing with geographic information, it is not rare to have to scan documents on paper or film. Because they are intended to be superimposed over Earth observation images, their geometry quality shall also be verified.

We distinguish basically three types of scanners:

- continuous feed – in which document is carried along by wheels to make it scroll in front of one or more CCD (« *Charged Coupled Devices* ») array(s);

– flat-bed – in which document is laid flat while a CCD array is moving over to scan the document;

– drum – in which document is attached over a drum rolling in front of a laser and CCD(s).

These three technologies enable processing documents of different sizes, and produce digital images of very different qualities. *Drum-scanners* are hardware that significantly enable reaching the highest resolution together with a high geometric quality but are expansive. *Continuous feed scanners* may process large documents, are rather cheap, but often produce deformations due to the friction of the wheels (see one example in figure X.8). *Flat-bed scanners*, except when they are very expensive, are only able processing small documents (A4 or A3).

2.1.4.2. Viewing models

We distinguish at least four basic types of viewing geometry from aerial or space platforms (see figure X.5).

- Conic – matches an instantaneous photography of the terrestrial surface (this mode is the one of most of the instruments onboard airborne) ;

- push-broom – in which a line of terrain across the flight line (also called NADIR) is seen with a constant scanning frequency (example of SPOT HRV) ;

- scanner – for which a oscillating CCD array scans the terrain from one side to the other one of the NADIR (example of Landsat TM) ;

- radar – analysing the go-return time and the phases of an emitted signal to one side of the NADIR.

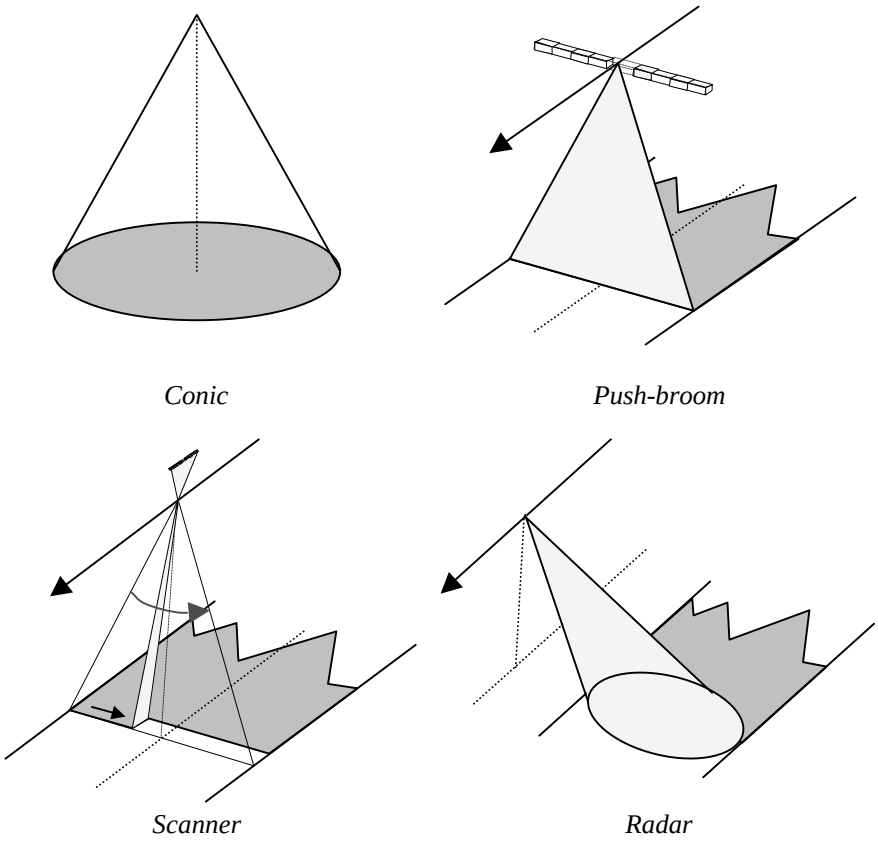

Figure X.5. Basic viewing technologies from platforms.

This list of acquisition types is not exhaustive. Other technologies exist, often more complex like the “TV-scanning” of Meteosat satellites or the “conic scanning” of the ATSR instrument on-board ERS and Envisat satellites…

Each technology leads to its own geometry defects that are presented in section 1.2.3.

Direct and/or inverse localisation functions may be complex. They are the expression of a viewing model involving the position of the platform, its instantaneous attitude (i.e. its orientation), the geometry of the instrument, and an Earth model that may possibly include an elevation model.

For example, figure X.6 illustrates one of the various reference frames used to model the acquisition of the HRV instrument onboard SPOT satellite.

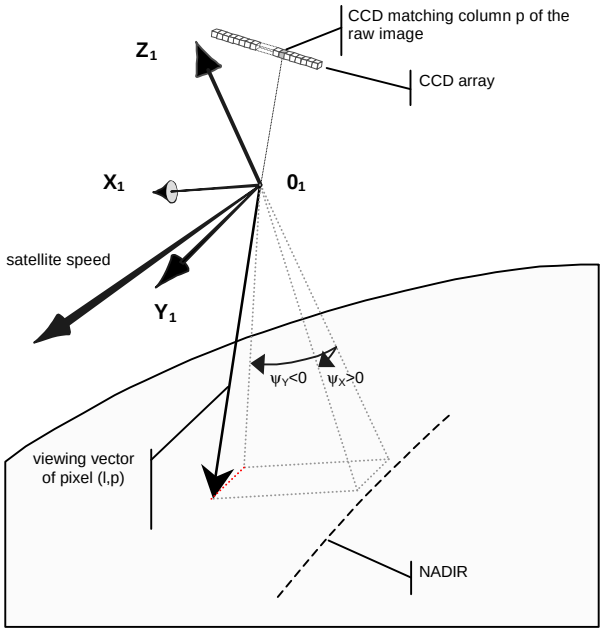

Figure X.6. Viewing vector within the "Navigation Reference Coordinate System" ("*Repère à piloter*" in French) of SPOT-HRV.

2.2. Definitions

We may notice a large confusion regarding the meaning of terms relative to image processing activities and in particular to their quality control. Mixing of French and English has increased such a confusion. Without claiming any exhaustiveness, definitions laid down in this section are an attempt at clarification as a complement to the definitions to be found in the dictionary [CON 97].

2.2.1. Georeferenced image

We call *georeferenced image* an image in which for any point (l,p), geodetic coordinates (λ,φ) or cartographic coordinates (X,Y) are given by an analytical formula or one algorithm (automate) as complex being (case of level 1A image of SPOT in the opposite figure).

The direct localisation function (eq. X.1) assumes this role; but other localisation functions may exist for a same image. For example, ancillary data of SPOT scenes provided with polynomial coefficients allowing to approximate this localisation function (case of level 1B image of SPOT in the opposite figure).

2.2.2. Geocoded image

We usually call *geocoded image* an image for which a linear direct localisation function exists giving the geodetic coordinates (λ,φ) or the cartographic (X,Y) for any point (l,p) of the image.

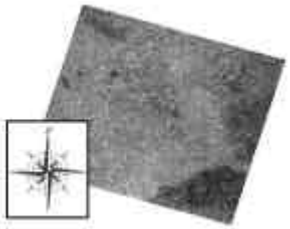

$$\begin{cases} X = X_0 + P_w \times p \\ Y = Y_0 - P_h \times l \end{cases} \quad [X.3]$$

Where

(l,p)	are the coordinates of the point in the image,
(X,Y)	are the cartographic coordinates or geodetic coordinates *(l, j),*
(X_0,Y_0)	are the coordinates of the upper-left corner,
P_w *and* P_h	are the on-ground width and height respectively.

2.2.3. Orthorectified image

We call *orthorectified image* an image for which parallax effects due to the relief and to the viewing vector (perspective effect) have been corrected. Orthorectification requires using a Digital Elevation Model (DEM). An orthorectified image is a geocoded image with cartographic accuracy.

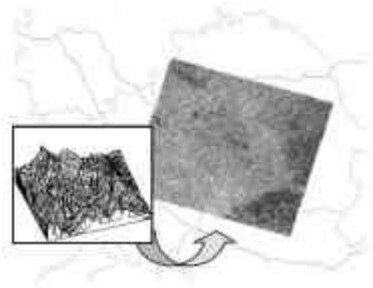

2.2.4. Check points

A *check point* (*point de contrôle* in French) is a quadruplet (l,p,Λ,ϑ) which geodetic coordinates (Λ,ϑ) have been provided by an external cartographic reference: -map, -geocoded image acting as reference, -GPS survey, -geodetic point… A check point is used to assess the localisation accuracy of the image to be checked.

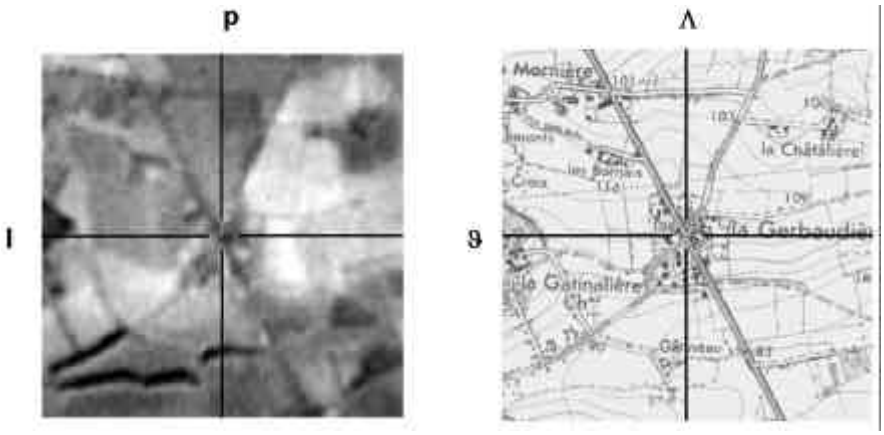

Figure X.7. Check point extracted from a map at a crossroads.

An accurate extraction of check points is a difficult exercise that depends on the scale of the documents, the type of objects found in the landscape (for example a crossroads is often more precise than a pier), the precision of the tool used to pick the point, the operator skills…

Nevertheless, we may enumerate some basic rules for the survey of check points:

- to favour intersections of nearly perpendicular axes (roads, field corners, building corners…) ;

- to display the zoomed image and the reference document at the same scale ;

- to dispatch check points in a homogeneous way within the image to be checked ;

- in mountainous areas, to get check points both at the bottom of valleys and on elevated zones (ridges and saddle points) ;

2.2.5. Tie points

A *tie point* (also called *GCP* or *control point* in English and *point d'appui* or *point de calage* in French) is a quadruplet (l,p,Λ,ϑ) extracted like a *check point* but that is used to register the direct localisation function, solving uncertainties linked to the unknowns of its attached model.

For example, if the location (X_S,Y_S,Z_S) of the platform is not known when the terrain has been imaged, at least three points are required to interpolate this location

using a technique called *triangulation*. From more tie points, we may refine this platform location minimising the mean quadratic error.

We may often notice a confusion between *check points* and *tie points*. This confusion is certainly due to the double semantic of the word “control” meaning at the same time “to assess the quality” and to “monitor the model”. In French language, the first meaning is more used while the second one seems to be favoured in English.

2.2.6. Localisation error

The *localisation error* of one point is the distance between the geodetic location (λ,φ) given by the direct localisation (eq. X.1) and the location (Λ,ϑ) observed in the surveyed check point.

$$e = dist[(l, j),(\Lambda, q)] \qquad [X.4]$$

Where

dist is the distance function to be defined: Euclidian distance or geodetic distance…

2.2.7. Mean quadratic error

The *mean quadratic error*, also called RMS (Root Mean Square) error, is a mean of the localisation errors.

$$rmse = \sqrt{\frac{1}{n}\sum_{i=1}^{n} e_i^2} = \sqrt{\frac{1}{n}\sum_{i=1}^{n} dist[(l_i, j_i),(\Lambda_i, q_i)]^2} \qquad [X.5]$$

Where

n is the number of check points,

e_i is the localisation error of point i (i=1..n),

$(l_i j_i)$ is the geodetic location computed by the direct localisation function applied to point i (i=1..n),

$(L_i J_i)$ is the geodetic location given by the reference cartographic document at point i (i=1..n),

dist is the distance function to be defined: Euclidian distance or geodetic distance…

2.2.8. Error vector field

Error vector of one point i joins the location $(l_i j_i)$ predicted by the direct localisation function (corrupted by an error) up to the $(L_i J_i)$ provided by the reference document (supposed to be the correct location).

$$\vec{v_i} = \begin{pmatrix} \Lambda_i - l_i \\ q_i - j_i \end{pmatrix} \qquad [X.6]$$

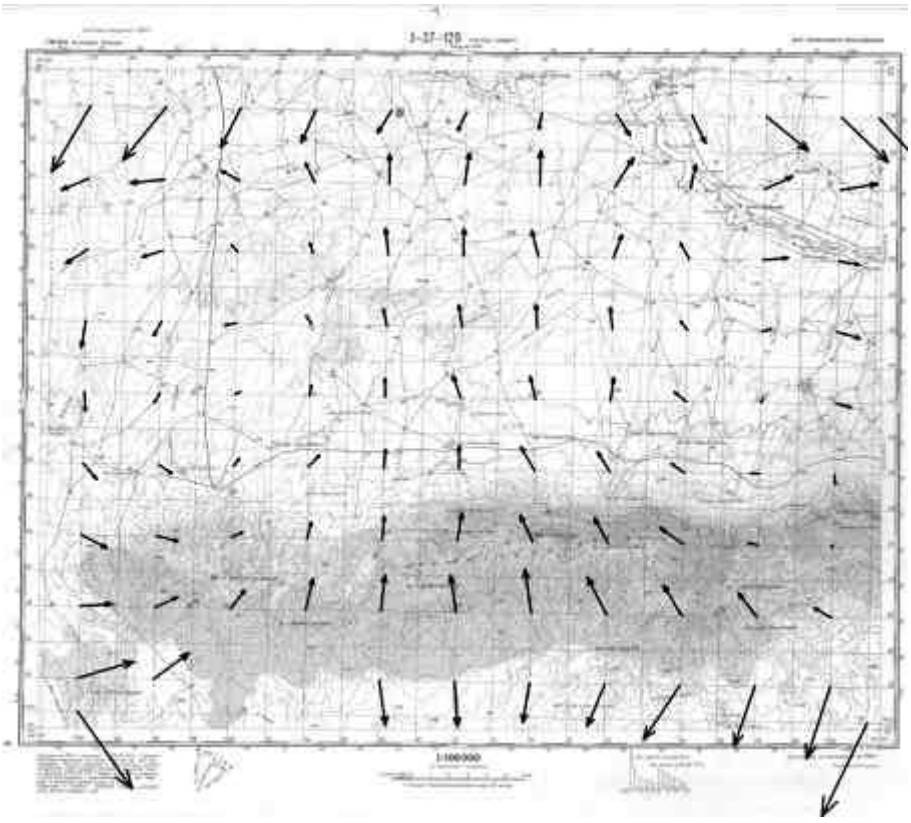

Figure X.8. Error vector field of a scanned map.

Displaying the error vector field is an excellent way to understand the defects of the direct localisation function. For example, figure X.8 illustrates the case of a paper map having been scanned by a continuous feed scanner whose wheels have caused extensions / compressions of the paper.

2.2.9. Native projection of a map

The *native projection of a map* is the reference coordinate system that has been used for its generation. Horizontal (X) and vertical (Y) axes of the native projection are strictly parallel to the map borders and graduations are spaced with a constant interval.

A map may include grids, tick marks, cross marks matching another projection, and sometimes many other projections.

When a map is scanned for geocoding, it is recommended to get a significant number of tie points (see for example figure X.8) regularly spaced and distributed within the image, and to transform this scanned image in its native projection using a polynomial interpolation of degree 2 and maximum 3 (too high degrees may lead to oscillations).

2.3. Some geometry defects

2.3.1. Absolute localisation defect

The algebraic mean of each component in latitude and longitude enables detecting a translation between the location $(l_i j_i)$ predicted by the direct localisation function and the location $(L_i J_i)$ given by the reference cartographic documents.

$$\begin{cases} \overline{m_l} = \frac{1}{n}\sum_{i=1}^{n}(\Lambda_i - l_i) \\ \overline{m_j} = \frac{1}{n}\sum_{i=1}^{n}(q_i - j_i) \end{cases} \qquad [X.7]$$

This vector (m_λ, m_φ) measures the *absolute location error*.

For images acquired by scrolling satellites, this defect is generally due to erroneous values of the platform ephemeris (giving the location and speed) and particularly in their attached timestamp (date/time).

For example, the opposite figure shows the location on Earth of a SPOT scene acquired by a lateral viewing and the terrestrial projection of the 8 ephemeris data contained in the product header. A timestamp error of these data would lead to move the location of the SPOT scene along a line parallel to the NADIR.

The absolute location error may easily be corrected just adding values m_λ and m_φ to the coordinates of the upper-left corner that is generally kept as auxiliary data of a geocoded image in almost all the Geographic Information Systems (GIS).

2.3.2. Global defects of internal geometry

Analysis of error vector directions may quickly enable detecting global deformations (called low-frequency deformations) of an image.

The absolute localisation error seen in the previous section is also a global deformation in which error vectors are almost parallel (figure X.9.a).

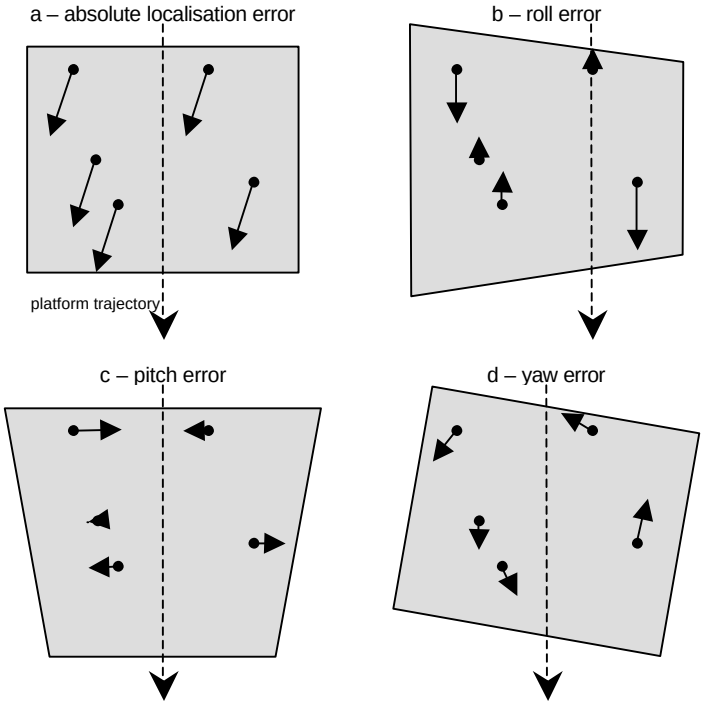

Figure X.9. Some global defects of internal geometry.

Defects of roll (b), pitch (c) and yaw (d) are due to uncertainties in the attitude of the platform (airborne or satellite) and therefore about the viewing direction that will intersect the Earth. Roll and pitch errors lead to perspective effects in the image while a yaw error leads to a rotation of the image.

Over areas with small relief variations, these defects may be corrected individually and very locally using low degree polynomial transforms.

In all the other cases, an accurate orthorectification shall integrate ephemeris data (location and speed) of the platform and its attitude data (roll, pitch and yaw angles around a reference frame linked to this platform). A time shall be attached to these data enabling to establish a relation to the time of the image line (case of push-broom or scanner viewing model) or to the instantaneous time of acquisition (case of conic viewing model).

2.3.3. Local defects of internal geometry

Local defects of internal geometry (called high-frequency deformations) may have different causes. Let us enumerate some of the most classical ones.

2.3.3.1. DEM accuracy

When an image is orthorectified, it shall be corrected of parallax defects (see figure X.10) that combine effects of the elevation α of the viewing vector with the elevation h of the terrain.

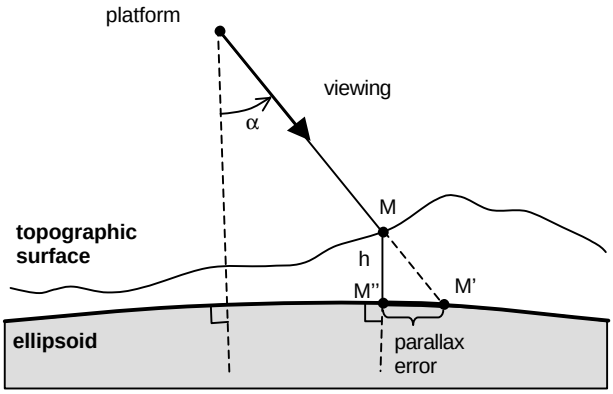

Figure X.10. Parallax error.

To be accurate, the parallax error is the geodetic distance (M',M''), measured along the ellipsoid, between the vertical projection M'' of point M on the ellipsoid and the intersection M' of the viewing vector with this ellipsoid. Nevertheless, this error may also be approximated using the simple formula :

$$\overline{M'M''} = h \times \tan(a) \qquad [X.8]$$

To be consistent, the viewing model and the Digital Elevation Model (DEM) shall make reference to the same terrestrial representation. We generally use the WGS84 ellipsoid. In particular, the DEM shall contain elevations with reference to the ellipsoid and not altitudes above the geoid that may differ from the WGS84 by up to 200 metres.

The quality of a Digital Elevation Model is defined by two measurements:

- *planimetric resolution* – which gives the on-ground spacing between two consecutive elevation values ;

- *elevation resolution (or vertical resolution)* – defining the vertical accuracy of elevation measurements (generally provided in metres or decimetres).

In orthorectified images , when the error vector direction depends on the elevation of the check points (see figure X.11), local defects of the internal geometry may be due to the accuracy of the DEM being used, or to an error in its geographic location, or to the interpolation method being used to estimate elevations in this DEM.

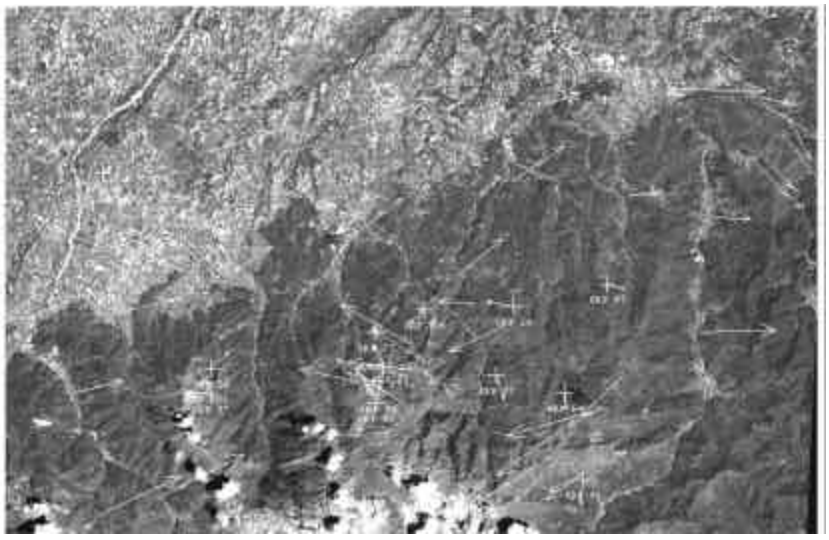

Figure X.11. Defects of parallax corrections in a mountainous area.

2.3.3.2. Defects due to the instrument

Push-broom instrument

Alignment of CCDs along its array, or the alignments of arrays between each other are strictly checked in laboratories before launch. Viewing angles of each

CCD are furnished to the processing facilities. These angles are used in viewing model, enabling facilities to compute the products that are distributed to users.

Because of launch conditions or simply because of ageing, we may observe differences between current values of these viewing angles and those measured before launch. Such variations are very complex to measure in order to correct the viewing model.

Figure X.12 shows for example an alignment defect along pixels in a wide field product. This defect has been detected analysing the disparities with a reference image.

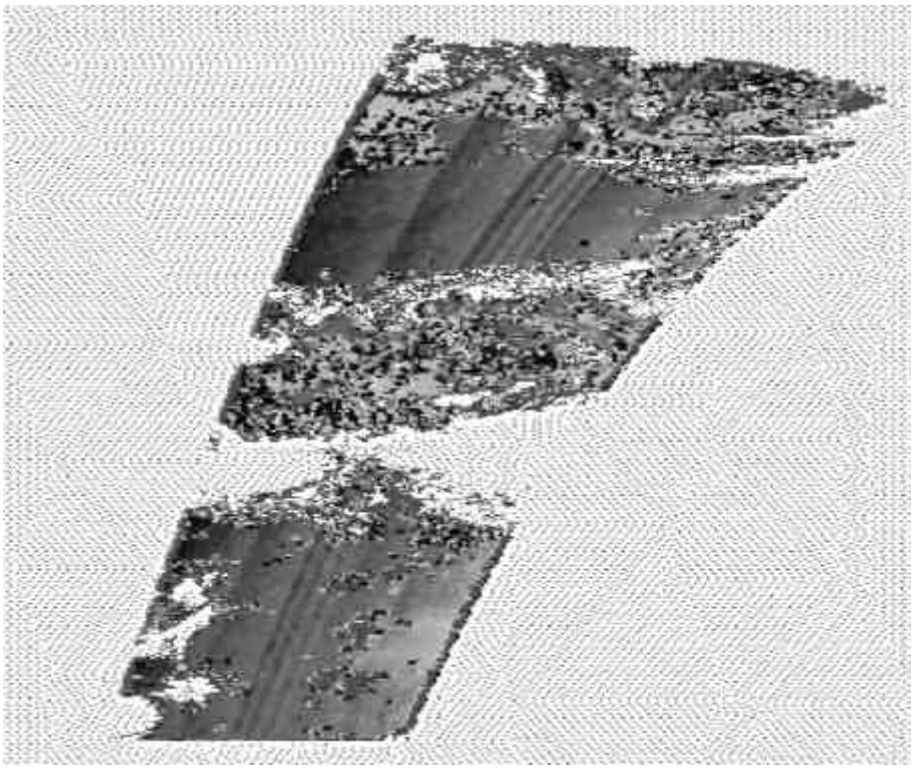

Figure X.12. Alignment defect along pixels of a wide field segment.

Scanner instruments

Acquisition by a scanner instrument (for example Landsat TM or ETM+) is performed by series of alternated scans (each one being called *swath*). To set successive scans as parallel as possible, the light path through the instrument is

deviated by lateral correcting mirrors. To reconstruct the image, each swath is interpolated by polynomials adjusted on three dates that are measured when the oscillating mirror crosses three internal cells.

Errors in the measurement of these dates may lead to a shift of one or more swaths towards the successive ones (see an example given in figure X.13).

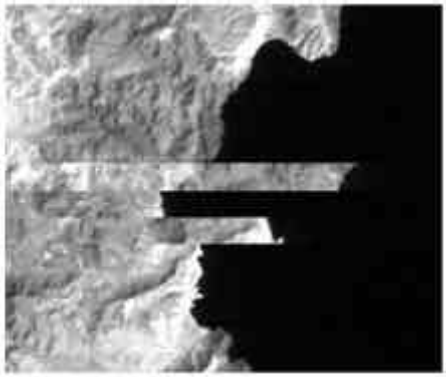

Figure X.13. Swath shift in a Landsat TM image
(Courtesy GAEL Consultant).

Other geometry errors have been observed in images acquired by a scanner instrument (see the non-exhaustive list given in figures X.14).

a – Displacement along line.

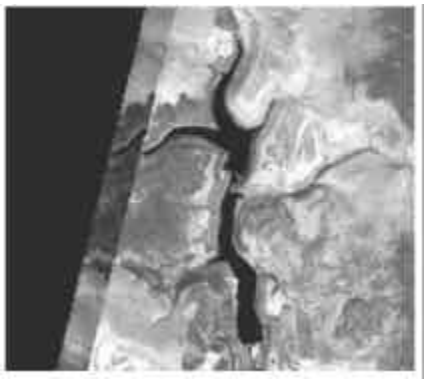

b – Shift of channels.

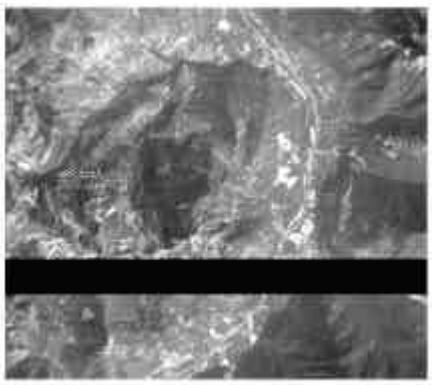

c – Lines or swath(s) lost.

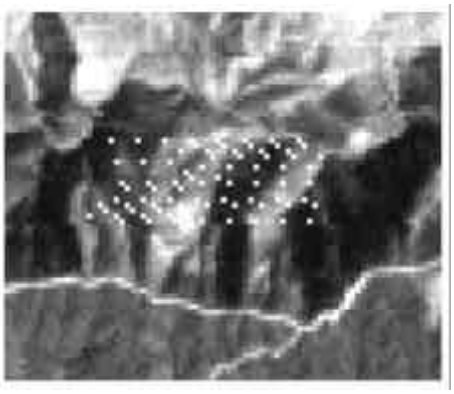

d – Pixels lost..

Figure X.14. Some defects observed in Landsat TM images
(Courtesy GAEL Consultant).

2.4. Localisation control and global models

Absolute location checks (§1.2.3.1), global defects (§1.2.3.2) or defects with a magnitude at least greater to one pixel may be processed using an application that enables getting check points (§1.2.2.4) and measuring the :

- quadratic mean of localisation errors (eq. X.5).
- arithmetic mean of localisation errors (eq. X.7).

To be significant, statistics shall be based on at least 20 check points regularly distributed in the image and using reference cartographic documents which quality and accuracy are themselves known.

2.5. Internal geometry control

Internal geometry checks shall enable detecting errors of sub-pixel size. This is for example required when assessing the CCD viewing angles verifying that viewing vectors intersect a plane tangent to the Earth according to a regular grid.

One of the most used method is the *disparity analysis* in which we look for matching points (or a subset of regularly spaced points) of the image to be checked with their homologous points in a reference image.

Such a matching is generally performed assessing the correlation between two windows (one in the image to be checked and the other one predicted in the

reference image). One of these windows is moved across an exploration window to find the value of the displacement (dx,dy) for which the correlation index is the highest one.

Disparity analysis produces two images: -one image of the vertical displacements (dx), and –one image of the horizontal displacements (dy). Sometimes a third image may be computed keeping the confidence index of each matching.

Figure X.15 for example shows results of a disparity analysis performed on one Landsat ETM+ scene orthorectified from one DEM with regard to the same Landsat scene orthorectified from an other DEM.

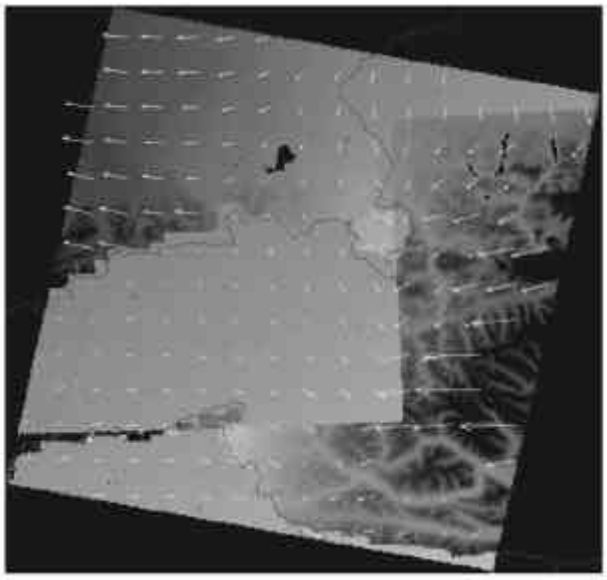

Figure X.15. Results of the disparity analysis on a Landsat ETM+ scene orthorectified with two different DEMs
(Courtesy GAEL Consultant).

As we may observe, disparity analysis may produce very fine results enabling to retrieve the limits of the DEMs that have been used for the orthorectification but also the relief (or more precisely the “anti-relief”) in zones where only one DEM has been used.

3. Radiometry quality

3.1 Radiometry quantities

The spectral domain of concern is the solar spectrum. Therefore, we exclude the thermal domain for which the concept of apparent temperature is introduced. The energy flux ϕ corresponds to an energy which can be emitted, received or transported per unit time and then expressed in Watts. We then define the density of energy flux (or net flux) as the energy flux which goes through an elementary surface.

$$F = \frac{df}{d\Sigma} \quad \left(W.m^{-2}\right) \qquad [X.9]$$

The radiance corresponds to the energetic flux which goes through an elementary surface $d\Sigma$, following a direction θ to the normal to the surface and contains in a solid angle $d\Omega$. This radiance is expressed as:

$$L = \frac{d^2 f}{d\Omega d\Sigma \cos q} \quad \left(W.m_{-2}.sr_{-1}\right) \qquad [X.10]$$

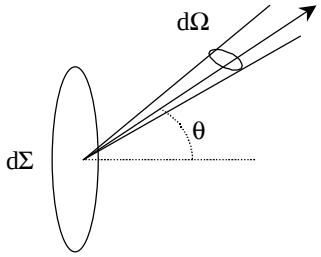

Figure X.16. Energetic flux through an elementary surface.

We introduce as well monochromatic radiance L_λ ($W.m^{-2}.sr^{-1}.\mu m^{-1}$):

$$L_l = \frac{dL}{dl} \qquad [X.11]$$

For a satellite sensor, accounting for the spectral response R_λ of the instrument, it is useful to introduce the concept of equivalent monochromatic radiance L_{eq} ($W.m^{-2}.sr^{-1}.\mu m^{-1}$):

$$L_{eq} = \frac{\int L_l R_l \, dl}{\int R_l \, dl} \qquad [X.12]$$

Let us consider a parallel beam of irradiance Es, lighting the elementary surface under an incident angle θ_s.

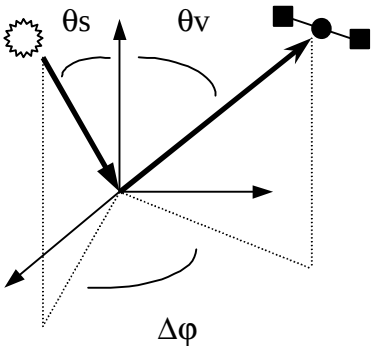

Figure X.17. The direct to direct path from Sun to satellite.

Let us consider the radiance $L(\theta_s,\theta_v,\Delta\varphi)$, reflected by the surface in a given direction, characterized by (θ_v, $\Delta\varphi$) (Figure X.17), the bi-directional reflectance is defined as:

$$r(q_s,q_v,\Delta j) = \frac{pL(q_s,q_v,\Delta j)}{m_s E_s} \qquad [X.13]$$

where μ_s is the cosine of the solar zenith angle θ_s. If ρ is constant whatever the incident angle and the reflection angle are, then the surface is lambertian and the reflected radiance is isotropic. If the reflectance is non-lambertian, a given target illuminated or viewed under different geometrical conditions does not give the same reflectance. Once can then normalize the observed reflectance to the one we should observe with the sun at zenith and for a nadir view. This normalization requires a

library of standard bi-directional models. The choice of the bi-directional model depends upon the type of surface. The surface classification can be conducted on colour images using a spectral index which is quite independent of the geometry.

3.2. Overview of the radiometric defects

We report here the various factors which affect the radiometric quality of the data, given some information about the applied corrections. The last example is more specific to aerial views.

3.2.1. Diffraction and defocalization

Using a schematic representation of the optics by a simple lens, an object point located at infinite only converges in the focal plane if the focussing of the instrument is perfect. On the other hand, because of diffraction, a point image corresponds actually to a small disk. These two defaults are generally well controlled.

3.2.2. Polarization of the instrument

The light is polarized: the intensity varies when rotating an analyser in front of a camera viewing a natural scene. On the other hand, the optics of one instrument polarized by itself: incident polarized light of same intensity gives different responses depending on the direction of polarization. Such a simple experiment enables describing the intrinsic polarization of one instrument. Therefore, having some idea about the degree of polarization of natural scenes, we can apply a first order correction of addition energy due to the instrumental polarization.

3.2.3. Stray light

Within the optical assembly, undesirable reflections occur on the different inside walls (surfaces) as well as on the optical gun even if all the surfaces are treated with anti blooming material. For ideal optics, a well collimated thin beam (as it is obtained from a laser beam) only lights an elementary detector. Practically, one can observe a spatial distribution of light on the full image. This light distribution is characterized by the *Point Spread Function* (PSF) which can be used then to correct for this stray light effect. This correction can be time consuming but it is a clear requirement to improve the radiometric quality.

3.2.4. *Aerial photo*

Aerial shots taken in conic geometry induce non-isotropic distribution of light densities in the image. Such an effect, called “*vignetting*” (“*vignettage* in French”)

generally produces darker corners or sometimes a decrease of the brightness from the centre to the image borders (see figure X.18).

Vignetting is due to the composition of atmosphere (humidity, aerosols, pollution…), to the focal length used (a greater aperture at 153 mm produces more vignetting than a 210 mm focal), to the altitude of flight (below 500 metres vignetting is less significant), to the location of the aircraft relatively to the 0°C inversion layer, to the attitude of the aircraft…

For better photographs, it is possible to use filters limiting the vignetting effect. Modern optic lenses are now available to compensate this defect.

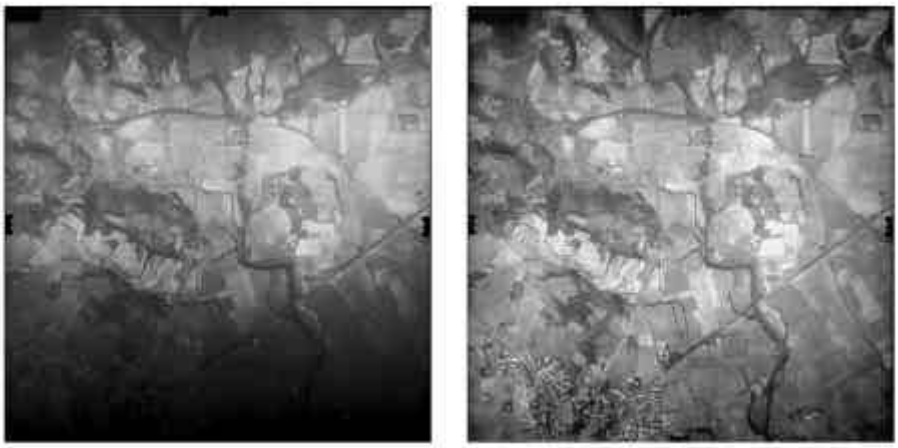

Figure X.18. *Raw aerial photo (left) and after vignetting correction (right). (Courtesy TTI Production, France)*

Many software tools enable correction of the vignetting defect. One of the most used consists in computing light distribution statistics both along lines and along columns, interpolating a polynomial correction function that will register radiometry on the one observed at the centre of the image (see figure X.18).

3.3. Calibration of the radiometric data

3.3.1. Radiometric calibration

The energy (in Joule) received by a sensor in converted into digital counts (DC). Even without any incoming light, digital counts DC_0 are recorded (dark current). This dark current is routinely measured by occulting the optics or, when it is not feasible, by measuring the dark signal (for example during night over the oceans or over desert areas).

The calibration consists in associating DC with the desired radiometric value. To do so, the DCs are recorded in circumstances for which the incoming signal is predictable. It can be achieved in the laboratory, in flight with an onboard calibration device or over targets for which the optical characteristics can be known (so called vicarious calibration).

3.3.1.1. Laboratory calibration

Standard calibrated sources are used (standard lamp, power supplied by a well controlled and stabilized current, and under theses conditions, stable during a given period of time) from which we accurately know the monochromatic irradiance ($W.m^{-2}.\mu m^{-1}$) at a given distance (generally one meter). This irradiance is transformed into radiance. Two main experimental settings are used:

(i) A perfectly reflecting sphere is equipped with one or several standard lamps. Multiple reflections within the sphere produce a perfect isotropic radiance which is accurately known. The sensor we want to calibrate views the interior of the sphere through a small hole. The bigger the sphere is and better the accuracy will be because the relative impact of the entrance hole will be reduced.

(ii) The standard lamp lights a white standard panel which is perfectly reflecting and almost lambertian (bi-directional properties of the panel reflectance are known for a second order correction). The distance between the lamp and the panel is well known in order to perfectly calculate the incident irradiance on the panel.

The advantages of the laboratory calibration are to offer well controlled conditions and to be repeatable. The accuracy decreases in the violet-blue spectral range with the sharp decrease of the lamp irradiances. If the calibration procedures are well conducted, once can expect to reach an absolute accuracy of 1% to 2%.

3.3.1.2. On-board calibration

Laboratory calibrations are regularly used for aircraft instrumentation and can be performed on request. We now have onboard calibration devices for satellite sensors. The sun is generally the direct source. Its light is reflected by a standard panel, well characterised in reflectance, in order to precisely know the incoming radiance to the sensor.

3.3.1.3. Vicarious calibration

In absence of on-board calibration, or to double check it, vicarious calibration is used to predict the incoming light. This prediction is generally done during dedicated field campaigns during which all the components of the signal are well quantified: surface reflectance, influence of the atmosphere,…

3.3.1. Spectral calibration

Most of the observations are multispectral and it is necessary to characterize the spectral response of each band (at least, the mean wavelength). A laboratory mono-chromator can be used for pre-flight characterization. Increasingly, spectrometer or hyperspectral instrument are used in space. For specific band settings, these instruments can aim to specific targets offering high spectral variabilities. It is primarily the case of the solar spectrum with the Fraunhoffer line. It is as well the case of well-defined atmospheric absorption lines (for instance the oxygen absorption around 761 nm). By matching these special spectral features, we can then achieve a vicarious spectral calibration.

3.4 Atmospheric correction

In a chapter devoted to the quality of the radiometric data, it is difficult to skip the problem of the atmospheric correction when the domain of interest concerns the surface. These atmospheric effects are major for oceanic observations: the atmospheric contribution represents between 60% and 80% of the signal. Land surfaces are more reflective. Nevertheless, the atmospheric correction is a key issue for images quality of the surface.

Let us use a simplified formulation of the signal to better understand the atmospheric correction problem :

$$r^* = T_g \left(r_{atm} + T_{atm}(m_s) \frac{r_G}{1 - r_G S_{atm}} T_{atm}(m_v) \right) \quad [X.14]$$

The gaseous transmittance T_g is associated to the ozone (Chapuis band between 0.55 um and 0.7 µm) and easy to correct for. Most of the spectral bands avoid the gaseous absorption and then T_g=1.

r_{atm}, T_{atm} and S_{atm} are respectively the atmospheric reflectance (the satellite signal observed over a dark target), the atmospheric transmitance (the attenuation of the light on the atmospheric path) and the spherical albedo (the proportion of the

light reflected by the surface and then backscattered downward). The atmosphere is composed by molecules for which the abundance (through the barometric pressure) and the scattering properties are well known (Rayleigh scattering). The molecular scattering is very effective in the blue. Complementary to the molecules, the aerosols present a large spatio-temporal variability. Therefore, we need to characterize them. Specific spectral bands, for which the surface contribution is minimum, are dedicated to aerosol remote sensing. They are located in the red and near infrared for oceanic observations. Over land, vegetation is used for aerosol remote sensing: vegetation is quite dark in the blue and in the red because of the photosynthesis. While the aerosols are characterized, atmospheric corrections schemes are applied.

The above atmospheric correction is relevant for an homogeneous Lambertian surface. The quality of the image is greatly improved and therefore atmospheric correction scheme are applied on operational basis. For coloured landscapes and high resolution pictures (of the order of few meters), the atmospheric effects are more complex because of the so-called adjacency effect.

4. Bibliography

[CON 97] CONSEIL INTERNATIONAL DE LA LANGUE FRANCAISE., « Terminologie de Télédétection et Photogrammétrie », *Editions PUF*, Paris ; 1997.

[RIA 02] RIAZANOFF S.., « *SPOT123-4-5 Geometry Handbook* », 82 pages; 35 figures; 32 equations ; SPOT IMAGE, Toulouse ; 2002.